REMOTE SENSING IMAGE COMPRESSION USING 3D-SPIHT ALGORITHM AND 3D-OWT

D. Napoleon

Assistant Professor, Department of Computer Science,
School of Computer Science And Engineering,
Bharathiar University,Coimbatore-641046
TamilNadu,India
mekaranapoleon@yahoo.co.in

S.Sathya

Research Scholar, Department of Computer Science,
School of Computer Science And Engineering,
Bharathiar University,Coimbatore-641046
TamilNadu,India.
selvarajsathya72@gmail.com

M.Praneesh

Research Scholar, Department of Computer Science,
School of Computer Science And Engineering,
Bharathiar University,Coimbatore-641046
TamilNadu,India.
raja.praneesh@gmail.com

M.Siva Subramanian

Research Scholar, Department of Computer Science,
School of Computer Science And Engineering,
Bharathiar University,Coimbatore-641046
TamilNadu,India.
sivasu4all@gmail.com

Abstract

Remote Sensing is the gathering of information about a place from a distance. Such information can occur by sensors or satellite, without making any direct contact with that object. We present a new technique for the compression of remote sensing images based on wavelet transform. This transform has similar complexity as the separable wavelet transform while providing better energy compaction and staying critically sampled, which makes it a good candidate for compression application. This paper focus on compressing the remote sensing images based on 3D-OWT scheme and 3D-SPIHT algorithm. Result show that our scheme with filters performs as well and better in lossless coding systems using 3D Oriented Wavelet Transform on remote sensing images.

Keywords**:** *Remote Sensing Image; Image Compression; Wavelet Transform; 3D-SPIHT.*

1. Introduction

Remote sensing in its broadest sense is simply defined as the observation of an object from some distance. Earth observation and weather satellites, medical x-rays for bone fractures are all examples of remote sensing. Remote sensing devices make use of emitted or reflected electromagnetic radiation from the object of interest in a certain frequency domain (infrared, visible light, microwave). Remote sensors are classified as either; active sensors or passive sensors. Active sensors provide their own source of radiation to send out to an object and record the magnitude of radiation returns. Passive sensors record incoming radiation that has been scattered, observed and transmitted from the earth in transmit from its original source, the sun.

Remote sensing images portray large areas of the earth at high spatial resolution and increasingly on a large number of spectral bands. As a consequence, they require huge resources for transmission to the ground station, archival and diffusion to the end users. For this reason, much attention has been devoted in recent years to the

compression of images. The major focus has been on transform coding based on Discrete Cosine Transform (DCT), Karhunen-Loeve Transform (KLT), or Discrete Wavelet Transform (DWT), followed by a suitable quantization step.

Quantization [1], [2] is theoretically the optimal block coding strategy. Indeed it is the direct application of the principles of information theory, and all other block coding techniques (e.g., transform coding) can be seen as structurally constrained forms of quantization. However, unconstrained quantization is characterized by a computational complexity that grows exponentially with the block size. As a consequence, practical coding schemes based on quantization are forced to use small block, thereby exploiting the statistical dependencies among only a small number of pixels and/or spectral bands. To obtain good encoding performance with limited complexity, many researchers rely on transform coding techniques [3]**,** where a linear transform decorrelates the input data concentrates most of the power in a few coefficients so that subsequent quantization is more efficient.

In the transform coding framework, wavelet transform [4], [5] deserves a special treatment because of its peculiar characteristics. Indeed due to its implementation as a recursive filtering procedure, it can easily work on large blocks there by providing an excellent power concentration. The Set Partitioning in Hierarchical Trees (SPIHT) algorithm [6] is one of the best wavelet based coding algorithm for remote sensing images. It is very efficiently exploits the self similarity between different levels in the wavelet pyramid and provides an embedded bit stream which support PSNR, MSE scalability. The excellent performance of SPIHT for remote sensing image makes it an attractive coding strategy. A 3D extension of SPIHT has been proposed by Kim and Pearlman in [7, 8]. They applied 3D wavelet transform and coded the wavelet coefficients by the 3D SPIHT algorithm.

Compression is a commonly used process to reduce the amount of initial data to be stored or transmitted by a channel to a receiver. In this paper, a transform will be introduced i.e., 3D-Oriented Wavelet Transform (OWT). In addition it is explored in image compression particularly for remote sensing images. Experimental results demonstrate that 3D-OWT can significantly improve the transform coding gain, particularly for remote sensing images with high resolution. In this paper we compare the proposed work using 3D SPIHT algorithm and 3D-OWT.

2. Methodology

Image Compression is one of the techniques in image processing. There are various types of Algorithms and techniques are used for compressed the images. Some of the Algorithms and techniques are SPECK Algorithm, SPIHT Algorithm, ASWDR Algorithm, LZW Coding, Fractal Coding. Here the proposed work is represented the architecture as shown the e.g. Fig. 1.

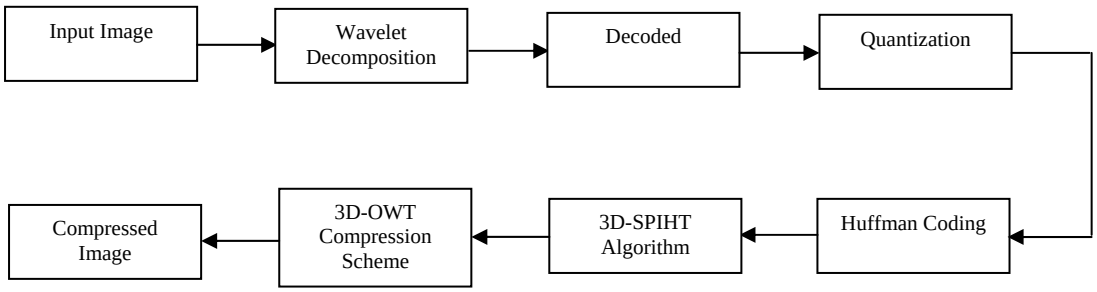

Fig. 1. System Architecture

3. The 3D-SPIHT Compression

The SPIHT algorithm is a highly refined version of the EZW algorithm. It was introduced by Said and Pearlman. Some of the best results highest PSNR values for given compression ratios for a wide variety of images have been obtained with SPIHT. Consequently, it is probably the most widely used wavelet based algorithm for image compression, providing a basic standard of comparison for all subsequent algorithms. SPIHT stands for Set Partitioning in Hierarchical Trees. The term Hierarchical trees refers to the quadtrees, Set Partitioning refer to the way these quadtrees divide up, partition, the wavelet transform values at a given threshold. The SPIHT algorithm proposed in this paper solves the spatial and temporal scalability trough the introduction of multiple resolutions dependent lists and a resolution dependent sorting pass. It keep important feature of the original SPIHT coder such as compression efficiency, full embeddedness, and rate scalability. The full scalability of the algorithm is achieved through the introduction multiple resolution dependent lists of the sorting stage of the algorithm. The idea of bitstream transcoding without decoding to obtain different bitstreams for various spatial and temporal resolutions and bit rates is completely supported by the algorithm.

SPIHT coding is applied on each band of the wavelet transform results to achieve compression. In order to take this fact into account, it is preferable to weight each band. As weight we use the energy $e = \sqrt{\sum_{x,y} b_\lambda(x,y)^2}/_{X.Y}$, where b_λ is the image band at the λ wavelength, X and Y and its dimension, and x and y are the position of a pixel in the band. Depending on energy band, we allocate proportional number of bits for the output of the SPIHT algorithm. The 3D approach consists in considering the whole remote sensing image as an input for full 3D decomposition. To achieve compression 3D SPIHT [9] is then applied.

The 3D SPIHT algorithm of [8] considers set of coefficients that are related through a parent offspring. In its bitplane coding process, the algorithm deals with the wavelet coefficients as either a root of an insignificant set, an individual insignificant pixel, or a significant pixel. It sorts these coefficients in three ordered lists: the list of insignificant sets (LIS), the list of insignificant pixels (LIP), and the list of significant pixels (LSP). The main concepts of the algorithm is managing these lists in order to efficiently extract insignificant sets in a hierarchical structure and identify significant coefficients which is the core of its high compression performance.

The 3D wavelet decomposition provides a multiresolution structure that consists of different spatio-temporal subbands that can be coded separately by a scalable encoder to provide various spatial and temporal scalabilities. In general by applying N_t levels of 1D temporal decomposition and N_s levels of 2D spatial decomposition, at most $N_s + 1$ levels of spatial resolution and $N_t + 1$ levels of temporal scalability are achievable. The total number of possible spatio-temporal resolution in this case is $(N_s + 1) + (N_t + 1)$. To distinguish between different resolutions levels, we denote the lowest spatial resolution levels as level $N_s + 1$ and the lowest temporal resolution level as N_t+1 . Algorithm provides full spatial and temporal scalability would encode the different resolution resolution subbands separately, allowing a transcoder or a decoder to directly access the data needed to reconstruct a desired spatial and temporal resolution.

4. 3D-Oriented Wavelet Transform

A novel technique of 3D-OWT that can perform three separable 1D transform in the arbitrary directions, including the same direction. The process behind this transform simply consists of applying the lifting steps of a 1D wavelet transform in the direction of the image contours. Using quincunx multiresolution sampling, the image is filtered along horizontal and vertical or diagonal and antidiagonal directions. This transform has similar complexity as the separable wavelet transform while providing better energy compaction and staying critically sampled, which makes it a good candidate for compression applications. The increased decorrelation offers relatively good performance compare to 3D-SPIHT algorithm.

4.1. *One Dimensilonal Wavelet Transform Based On Oriented Resampling*

For traditional DWT, it contains a pair of low pass and high pass filters, followed by downsampling by a factor of two after each filtering operation [10]. The filtering operation appears to be convolution between filter taps and image data. A two channel multirate filter bank convolves a signal a_0 with a low pass filter $\bar{h}[n] = h[n-1]$ and a high pass filter $\bar{g}[n] = g[-n]$ and downsamples the output by 2 as

$$a_1[n] = \sum_{m=-\infty}^{+\infty} h[m-2n]\, a_0[m] = a_0 * \bar{h}\,[2n]$$

$$d_1[n] = \sum_{m=-\infty}^{+\infty} g[m-2n]\, a_0[m] = a_0 * \bar{g}\,[2n]$$

The low pass convolution object of analysis filter is shown in the below figures. The fork and circle in this figures stands for the odd and even columns of data, and the bold box is a window for data to participate in the convolution.

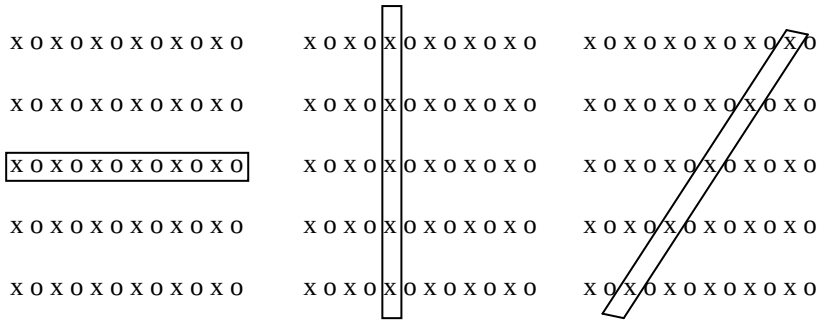

Fig. 2. Horizontal, Vertical and Diagonal Wise transform

Although 3D OWT can also be separated into three 1D trandforms based on oriented resampling, these three transforms are not essentially perpendicular. Once the first transform direction can be decided, the $a_0[n]$ should perform the oriented resampling in this direction. For instance, supposing that the first transform direction number is 4. The oriented resampling process for horizontal, vertical and diagonal wise transform is shown in e.g. Fig. 2. Nine resampled data along the diagonal direction become a substitution of $a_0[n]$, which perform convolution operation with the low frequency filter taps. Because the direction number is 4, there is no need for a subpixel. In some other directions, subpixels should be interpolated.

4.2. *Wavelet and Lifting*

Given a signal $s(t)$, the dyadic wavelet transform consists in representing S by its decomposition on a wavelet basis $\{\psi_{k,n}\}_{k\in\mathbb{N},n\in\mathbb{Z}}$

$$\Psi_{k,n}(t) = \frac{1}{\sqrt{2^k}}\Psi\left(\frac{t-2^k n}{2^k}\right),$$

$$S(t) = \sum_{k,n} c_{k,n}\,\Psi_{k,n}(t)$$

where $\Psi(t)$ is the *mother wavelet* and $\Psi_{k,n}(t)$ are scaled and shifted versions of this wavelet. We consider only biorthogonal and compactly supported wavelets. This ensures both the linear phase and perfect reconstruction property. Additionally, the transform can be implemented efficiently using a two-channel FIR filterbank, iterated on the low-frequency band. In [11], *et al* prove that the polyphase matrix of such a filterbank can be factorized in a finite number of predict (P_i) and update (U_i) steps, followed by a final scaling step (K). This lifting decomposition generalizes the notion of wavelets and allows the construction of second generation wavelets on sets where the notion of frequency is not defined [12]. Furthermore, the lifting scheme provides an efficient way of implementing the filterbank and guarantees perfect reconstruction by simple inversion of the different lifting steps. The number of predict and update steps depends on the regularity of the wavelet.

The analysis stage is performed by first splitting the sampling grid in two cosets.

$$C_1 \begin{cases} S_0[n] \coloneqq S[2n], \\ S_1[n] \coloneqq S[2n+1] \end{cases}$$

A predict step consists in predicting each sample of S_1 from its neighbours in S_0

$$P(\alpha_i) \coloneqq S_1 1\,[n] + \alpha_i\,(S_1 0\,[n] + S_1 0\,[n+1]$$

where α_i represents the lifting factor of the predict step i. Similarly, an update step consists in adjusting the value of each sample in S_0 from its neighbours in S_1

$$U(\beta_i) \coloneqq S_1 1\,[n] + \beta_i\,(S_1 0\,[n] + S_1 0\,[n+1]$$

where β_i represents the lifting factor of the update step i.

The predict and update steps are applied successively in alternance. To obtain properly normalized filters, a final scaling step is applied on each coset as

$$K(x) \begin{cases} S_0[n] \coloneqq xS_0[n] \\ S_1[n] \coloneqq \frac{1}{x}S_1[n] \end{cases}$$

S_0 is an approximation of S and corresponds to a lowpass filtering followed by downsampling, while S_1 represents the prediction error and corresponds to a high-pass filtering followed by downsampling. The original signal S is recovered by inverting the lifting steps, that is, by applying successively

$$R\left(\frac{1}{\alpha}\right), U(-\alpha_{N-1}), P(-\beta_{N-1}),\ldots,U(-\alpha_0), P(-\beta_0)$$

and merging S_0 and S_1 as

$$C^{-1}:\begin{cases} S[2n] := S_0[n] \\ S[2n+1] := S_1[n] \end{cases}$$

OWT performs a compression process of a signal or an image, using a wavelet packet. The procedures for compression using the wavelet packet decomposition are the same as those used in the wavelet framework. The DWT is an important tool in the construction of resolution scalable bit streams. First DWT stage decomposes the image into four sub bands, denoted LL_1, HL_1 [Horizontally High-pass], LH_1 [Vertically High-pass] and HH_1. The next DWT stage decomposes this LL_1 sub band into four more sun bands denoted LL_2, LH_2, HL_2 and HH_2. The process continues for some number of strategies. The total number of sample in all sub bands is identical to the original image. On comparing between 3D-SPIHT and 3D-OWT better compression ratio for Remote Sensing Images is obtained for 3D-OWT.

5. Image Quality Measurements

5.1. *Mean Square Error (MSE)*

The simplest of image quality measurement is Mean Square Error (MSE). The large value of MSE means that image is poor quality [13]. MSE is defined as follow:

$$\text{MSE} = \frac{1}{MN}\sum_{m=1}^{M}\sum_{n=1}^{N}\left(x(m,n)-\hat{x}(m,n)\right)^2$$

5.2. *Peak Signal to Noise Ratio (PSNR)*

The small value of Peak Signal to Noise Ratio (PSNR) means that image is poor quality. In general, a good reconstructed image is one with low MSE and high PSNR [13].PSNR is defined as follow:

$$\text{PSNR} = \frac{10\log 255^2}{MSE}$$

5.3. *Correlation*

Correlation coefficient quantifies the closeness between two images. The correlation coefficient is computed by using the following equation [14].

$$Corr\left(\frac{A}{B}\right) = \frac{\sum_{i=1}^{M}\sum_{j=1}^{N}\left(A_{i,j}-\bar{A}\right)\left(B_{i,j}-\bar{B}\right)}{\sqrt{\sum_{i=1}^{M}\sum_{j=1}^{N}\left(A_{i,j}-\bar{A}\right)^2\sum_{i=1}^{M}\sum_{i=1}^{N}\left(B_{i,j}-\bar{B}\right)^2}}$$

A correlation is a number between -1 and +1 that measures the degree of association between two variables (call them X and Y). A positive value for the correlation implies a positive association (large values of X tend to be associated with large values of Y and small values of X tend to be associated with small values of Y). A negative value for the correlation implies a negative or inverse association (large values of X tend to be associated with small values of Y and vice versa).

5.4. *Structural Similarity Measures*

The structural similarity (SSIM) index is a method for measuring the similarity between two images [15]. The measure between two windows x and y of common size N×N is:

$$SSIM(x,y) = \frac{(2\mu_x\mu_y + C_1)(2\sigma_{xy} + C_2)}{(\mu_x^2 + \mu_y^2 + C_1)(\sigma_x^2 + \sigma_y^2 + C_2)}$$

where μ_x is the average of x, μ_y is the average of y, $\sigma^2 x$ is variance of x, $\sigma^2 y$ is variance of y, σ_{xy} represents the covariance of x and y, $c_1=(k_1 L)^2$, $c_2=(k_2 L)^2$ two variables to stabilize the division with weak denominator.

5.5. *Execution Time*

The execution time for all the images are tested and compared with 3D-SPIHT and 3D-OWT which are used. The 3D-OWT gives the higher results for all the Remote Sensing Images. Execution time is calculated using tic toc method.

6. Dataset Description

Remote sensing image is defined as an image produced by a recording device that is not in physical or intimate contact with the object under study [16]. Remote sensing image is used to obtained information about a target or an area or phenomenon through the analysis of certain information which is obtain by the remote sensing imagery generally require correction of undesirable sensor characteristics and other disturbing effects before performing data analysis. Images obtained by satellite are useful in many environmental applications such as tracking of earth resources, geographical mapping, prediction of agriculture crops, urban growth, weather, flood and fire control etc. When capturing image using sensors, the resulting image may contain Noise from dirtiness on the image data acquisition process. So in this paper, we have analysed a remote sensing image. It is downloaded from Google sites.

7. Results

The figures show the experimental results of the proposed work. The test image is taken as Input image. It has very high frequency components, so the 3D-SPIHT algorithm and 3D-OWT technique is used to compress the Image. Both of the Algorithm and Technique compress the image. When compared to the 3D-SPIHT, 3D-OWT produces better compression which is shown in e.g. Fig. 3. This shows that the 3D-OWT has shown good efficiency for image compression. The proposed work is done using MATLAB, 2010 version.

Remote Sensing Image

Remote Sensing Image

Remote Sensing Image

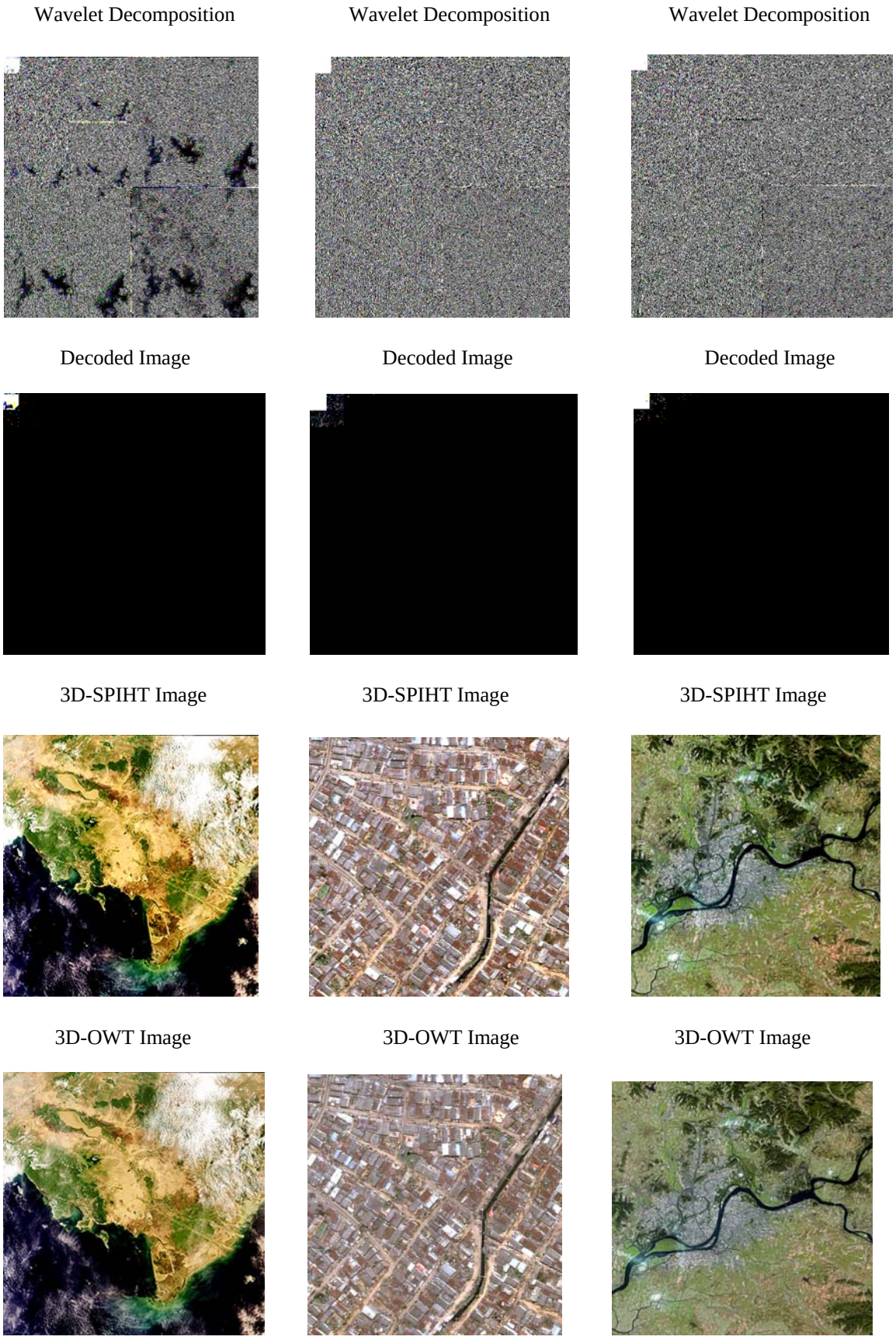

Fig. 3. Compression of 3D-SPIHT and 3D-0WT

Table 1. Results of CR, PSNR, MSE, Correlation, SSIM, Execution Time Value for 3D-SPIHT Algorithm.

3D-SPIHT ALGORITHM						
IMAGES	**CR**	**PSNR**	**MSE**	**CORRELATION**	**SSIM**	**EXECUTION TIME**
Image1	1.2095	28.5629	90.5297	0.9968	0.8326	29.4804
Image2	1.0199	27.7763	108.5040	0.9873	0.9017	21.0090
Image3	1.0046	31.3066	48.1310	0.9890	0.8502	41.4331
Image4	0.9993	29.7236	69.2972	0.9917	0.8602	35.2268
Image5	0.9990	29.6854	69.9110	0.9932	0.9048	31.7721

Table 2. Results of CR, PSNR, MSE, Correlation, SSIM, Execution Time Value for 3D-OWT.

3D-OWT						
IMAGES	**CR**	**PSNR**	**MSE**	**CORRELATION**	**SSIM**	**EXECUTION TIME**
Image1	0.9727	37.7164	11.0012	0.9991	0.9791	0.1869
Image2	1.0067	33.0596	32.1458	0.9868	0.9128	0.1835
Image3	1.0090	35.4889	18.3736	0.9937	0.9431	0.1834
Image4	1.0089	35.1416	19.9031	0.9921	0.9337	0.1863
Image5	1.0092	34.3174	24.0623	0.9934	0.9505	0.1839

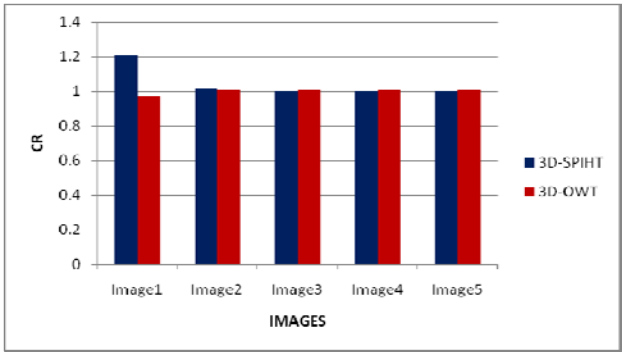

Fig. 4. Comparison of CR in 3D-SPIHTand 3D-OWT

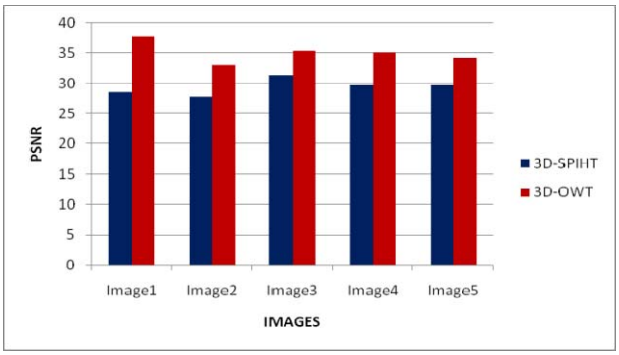

Fig. 5 . Comparison of PSNR in 3D-SPIHT and 3D-OWT

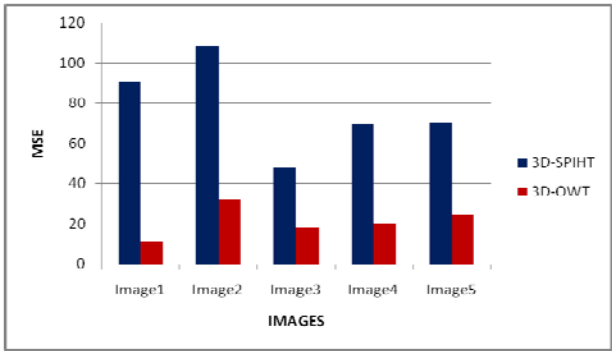

Fig. 6. Comparison of MSE in 3D-SPIHT and 3D-OWT

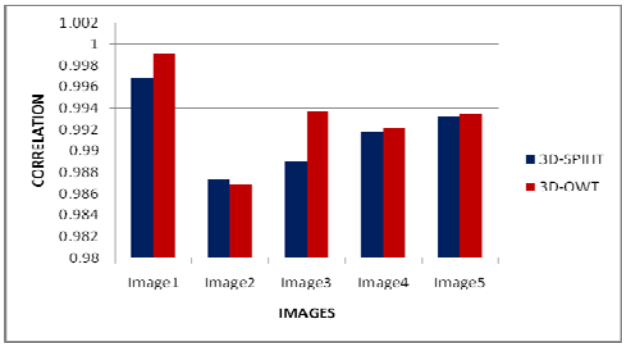

Fig. 7. Comparison of Correlation in 3D-SPIHT and 3D-OWT

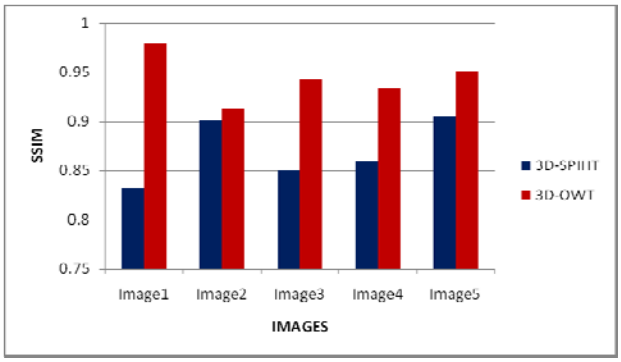

Fig. 8. Comparison of SSIM in 3D-SPIHT and 3D-OWT

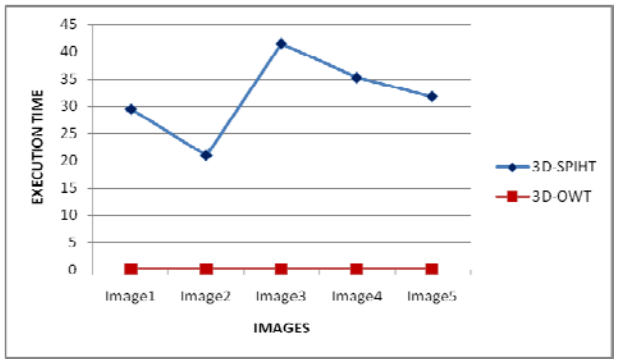

Fig. 9. Comparison of Execution Time in 3D-SPIHT and 3D-OWT

8. Conclusion

In this paper, we compared 3D-SPIHT algorithm and 3D-OWT compression scheme for the compression of remote sensing images. The compression algorithm based on the proposed transform can achieve superior quality of decoded images. The proposed transform provides a combination of oriented information and wavelet transform. 3D-OWT has some complexity as same that of wavelet transform but even though it provides better energy compaction and staying critically sampled, which makes it a good candidate for compression applications. Our experiment shows as 3D-OWT compression scheme is suitable for remote sensing image compression compared with the 3D-SPIHT algorithm.

References

[1] A. N. Netravali and B. G. Haskell, Digital Pictures, Representation and Compression. New York: Plenum, 1988.

[2] . Makhoul, S. Roucos, and H. Gish, "Vector quantization in speech coding," Proc. IEEE, vol. 73, pp. 1551–1588, Nov. 1985.

[3] A. Gersho and R. M. Gray, Vector Quantization and Signal Compression. Norwell, MA: Kluwer, 1992.

[4] S. Mallat, "Multifrequency channel decompositions of images and wavelet models," IEEE Trans. Acoust., Speech, Signal Processing, vol. 37, pp. 2091–2110, Dec. 1989.

[5] M. Vetterli and J. Kovacevic, Wavelets and Subband Coding. Englewood Cliffs, NJ: Prentice-Hall, 1995.

[6] A. Said and W. **A.** Pearlman, "A new, fast and efficient image codec based on set partitioning in hierarchical trees," IEEE Trans. Circ. and Syst. for video Technology. vol. 6, pp. 243-250, June 1996.

[7] B.-J.Kim and W. A. Pearlman, ''An embedded video coder using three-dimensional set partitioning in hierarchical trees (SPIHT)," inproc. IEEE Data Compression Con$, Mar. 1997, pp. 251-260.

[8] B.-J. Kim, Z. Xiong, and W. A. Pearlman, "Low hitrate scalable video coding with 3-d set partitioning in hierarchical trees (3-D SPIHT)," IEEE Trans. Circ. and Syst. for video Technology, vol. 10, no. 8, pp. 1374-1387,Dec. 2000.

[9] L. Dragotti, G. Poggi, A.R.P. Ragozini, "Compression of multispectral images by three-dimensional SPIHT algorithm". IEEE Transactions on Geoscience and Remote Sensing 38(1), 2000, pp. 416-428.

[10] S. Mallat, A Wavelet Tour of Signal Processing, 2nd ed. Singapore: Elsevier, 2003.

[11] Daubechies and W. Sweldens, "Factoring wavelet transforms into lifting steps," in *J. Fourier Anal. Appl.*, vol. 4(3), 1998, pp. 247–269.

[12] W. Sweldens, "The lifting scheme: A construction of second generation wavelets," *SIAM J. Math. Anal.*, vol. 29, no. 2, pp. 511–546, 1997.

[13] James S. Walker, "Wavelet-based Image Compression", Transforms and Data Compression.

[14] Wang, Z.; Bovik, A.C.; Lu, L., (2002). Why is Image Quality Assessment So Difficult? IEEE International Conference on Acoustics, Speech, & Signal Processing, 4, pp. IV-3313 - IV-3316.

[15] Zhou Wang, Alan C. Bovik, Hamid R. Sheikh, And Eero P. Simoncelli, "Image Quality Assessment: From Error Measurement To Structural Similarity", IEEE Transactions On Image Processing, Vol. 13, No. 1, January 2004.

[16] V.H Singhory ,D.D Nebert and A.L Johnson, Remote sensing and GIS for Site Characterization Application and Standard, American Society for Testing and Materials.